JOURNAL OF NEUROPHYSIOLOGY
Vol. 57, No. 2, February 1987. *Printed in U.S.A.*

# Cat Hindlimb Motoneurons During Locomotion. II. Normal Activity Patterns

J. A. HOFFER, N. SUGANO, G. E. LOEB, W. B. MARKS, M. J. O'DONOVAN, AND C. A. PRATT

*Laboratory of Neural Control, National Institute of Neurological and Communicative Disorders and Stroke, National Institutes of Health, Bethesda, Maryland 20892*

## SUMMARY AND CONCLUSIONS

*1.* Activity patterns were recorded from 51 motoneurons in the fifth lumbar ventral root of cats walking on a motorized treadmill at a range of speeds between 0.1 and 1.3 m/s. The muscle of destination of recorded motoneurons was identified by spike-triggered averaging of EMG recordings from each of the anterior thigh muscles. Forty-three motoneurons projected to one of the quadriceps (vastus medialis, vastus lateralis, vastus intermedius, or rectus femoris) or sartorius (anterior or medial) muscles of the anterior thigh.

*2.* Anterior thigh motoneurons always discharged a single burst of action potentials per step cycle, even in multifunctional muscles (e.g., sartorius anterior) that exhibited more than one burst of EMG activity per step cycle.

*3.* The instantaneous firing rates of most motoneurons were lowest upon recruitment and increased progressively during a burst, as long as the EMG was still increasing. Firing rates peaked midway through each burst and tended to decline toward the end of the burst.

*4.* The initial, mean, and peak firing rates of single motoneurons typically increased for faster walking speeds.

*5.* At any given walking speed, early recruited motoneurons typically reached higher firing rates than late recruited motoneurons.

*6.* In contrast to decerebrated cats, initial doublets at the beginning of bursts were seen only rarely. In the 4/51 motoneurons that showed initial doublets, both the instantaneous frequency of the doublet and the probability of starting a burst with a doublet decreased for faster walking speeds.

*7.* The modulations in firing rate of every motoneuron were found to be closely correlated to the smoothed electromyogram of its target muscle. For 32 identified motoneurons, the unit's instantaneous frequencygram was scaled linearly by computer to the rectified smoothed EMG recorded from each of the anterior thigh muscles. The covariance between unitary frequencygram and muscle EMG was computed for each muscle. Typically, the EMG profile of the target muscle accounted for 0.88–0.96 of the variance in unitary firing rate. The EMG profiles of the other anterior thigh muscles, when tested in the same way, usually accounted only for a significantly smaller fraction of the variance.

*8.* Brief amplitude fluctuations observed in the EMG envelopes were usually also reflected in the individual motoneuron frequencygrams.

*9.* To further demonstrate the relationship between unitary frequencygrams and EMG, EMG envelopes recorded during walking were used as templates to generate depolarizing currents that were applied intracellularly to lumbar motoneurons in an acute spinal preparation. By adjusting the resting membrane potential and the scale factor from voltage to current, impaled motoneurons could be made to generate bursts of action potentials that closely resembled the bursts recorded from motoneurons when the EMG records had been originally obtained.

*10.* We conclude that in unifunctional muscles, the fluctuations normally observed in EMG reflect ongoing changes in a central driving function that is common to the entire active motoneuron pool. This result suggests that, in unifunctional muscles, the whole-muscle EMG signal can provide accurate and

rather detailed information about the net input to the motoneuron pool. We find no need to postulate special pathways for recruitment of the different motoneurons activated during walking. Active motoneurons appear to differ only by their intrinsic thresholds and the strength of inputs that are common to the motor pool during this task.

## INTRODUCTION

The input-output properties of mammalian motoneurons have been extensively studied for cat lumbar motoneurons projecting to the hindlimb musculature (reviewed in 4, 5, 15, 38). Intracellular current injection has been used to study the effect of synaptic input on the discharge of individual motoneurons (e.g., 1, 2, 27). Until recently, however, relatively little was known about how motoneurons actually fire during movements. The development of the mesencephalic cat preparation provided the opportunity to record the discharge of hindlimb motoneurons during controlled locomotion on a moving belt (36, 42) as well as in the paralyzed "fictive" case (24, 25, 32). The natural firing patterns of cat hindlimb motoneurons during normal locomotion, however, had not been observed due to technical difficulties in obtaining secure motoneuron or motor-unit recordings in moving animals.

This paper presents a study of the natural activity patterns of individual motoneurons innervating cat anterior thigh muscles recorded during normal walking on a motorized treadmill. The methodological approaches to recording extracellular potentials from single motoneurons, identifying the muscle of destination, measuring axonal conduction velocity, and determining the unitary recruitment threshold are described in a companion paper (18). Two other papers address the special case of sartorius motoneurons that were found to be partitioned into three independent locomotor task groups (19) and the reflex responses of anterior thigh motoneurons to cutaneous inputs during locomotion (28). Preliminary reports have been published (20–22, 39).

## METHODS

The electrodes used to record the activity of single motor axons and the electromyogram (EMG) of individual cat hindlimb muscles are described in a companion paper (18). We detail here the processing of the signals recorded during locomotion and the analytical approaches used to evaluate properties of the discharge patterns of single motoneurons.

### *Selection of units for analysis*

We selected for this study 43 of 164 ventral root units recorded from 9 cats, based on the following requirements: the unitary recordings from the ventral root fiber were of sufficient quality to ensure accurate spike isolation from the raw microelectrode record; axonal conduction velocity was obtained from spike-triggered averaging of femoral nerve cuff records; bipolar recordings of the EMG from the target muscle were available; the recordings were obtained as cats walked at several different treadmill speeds. In addition, we analyzed in detail the discharge patterns of two motor units that were discriminated from the EMG of the medial portion of sartorius and we included them in this sample.

### *Determination of target muscle by spike-triggered averaging*

The electromyograms were obtained by indwelling bipolar electrodes (18) from the four heads of quadriceps (vastus intermedius, VI; vastus medialis, VM; vastus lateralis, VL; rectus femoris, RF) plus the anterior and medial portions of sartorius (SA-a, SA-m). EMG signals were amplified, filtered (0.05–5 kHz), and recorded on magnetic tape (DC-10-kHz bandpass) along with ventral root (VR) microelectrode recordings, femoral nerve cuff recordings, analog records of muscle length and muscle force, treadmill speed, and a master time code from an IRIG-B time code generator/translator (Datum 9300-100).

Spike-triggered averaging was performed either on-line or by retrieving data from magnetic tape. The natural discharge of a single VR axon, recorded by a microelectrode during walking, was isolated using a threshold and window discriminator (similar to Bak DIS-1). Each occurrence of a discriminated spike triggered the sweep of a four-channel signal averager (Nicolet 1174). The VR record and three of the six anterior thigh EMG records were delayed 1–5 ms using a pretrigger buffer and each channel was sampled by the averager every 20 $\mu$s. The procedure was then repeated for the same VR record and the EMGs from the three remaining anterior thigh muscles. Between 512 and 2,048 sweeps were usually needed to resolve single motor-unit potentials reproducibly and convincingly. Examples were given in a companion paper (Ref. 18, Fig. 5). Reproducibility of spike-triggered averages was always verified by the results of partial accumulations during repeated averaging and by subsequent averaging of different data segments.

### *Data acquisition*

Figure 1 summarizes the data processing steps and the numerical parameters rendered by the mathematical fitting approach we used. Consecutive

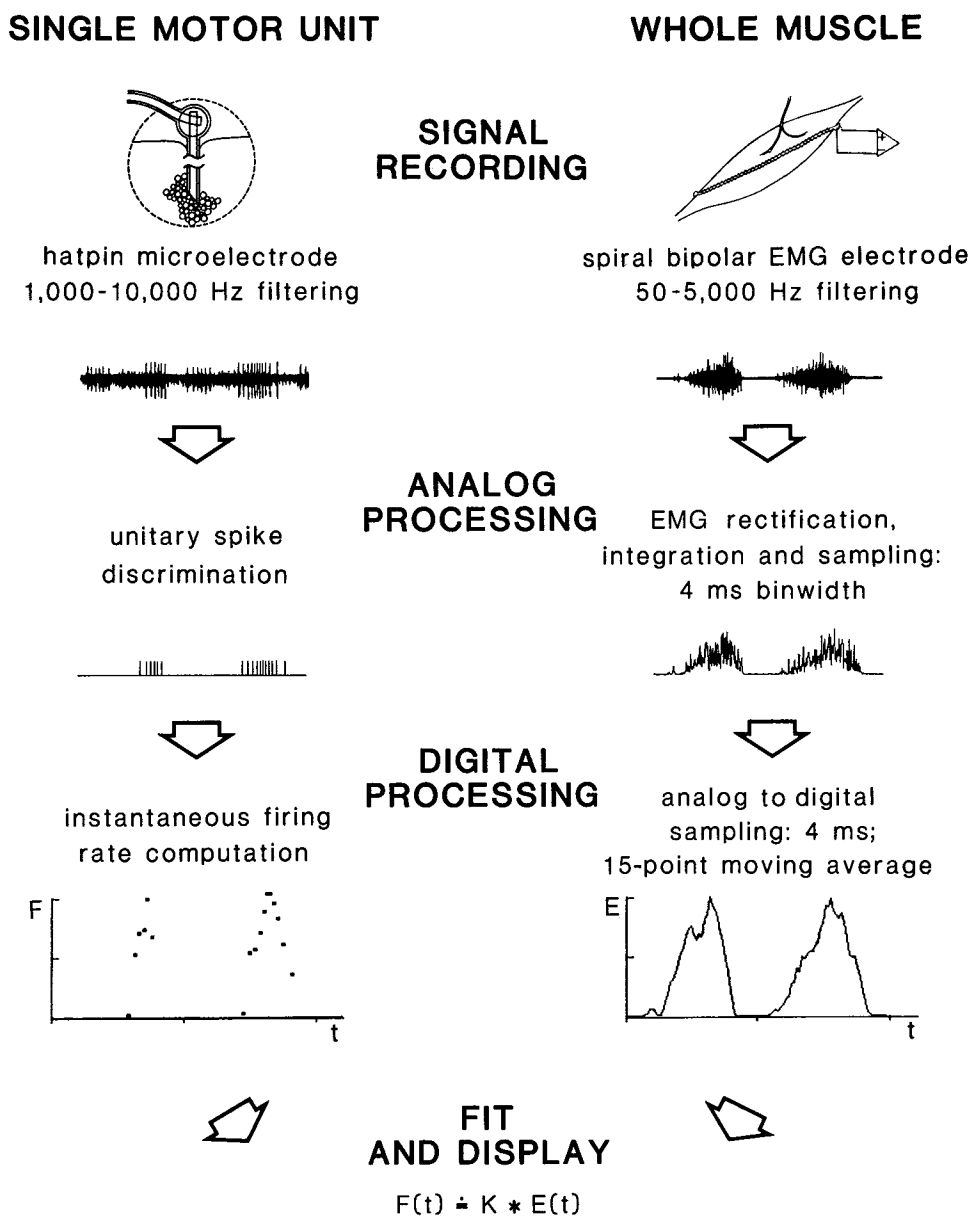


FIG. 1. Schematic diagram of the methodology used for recording, processing, and analyzing mathematically the locomotory activity patterns of single motoneurons and the EMG of their target muscles.

panels show the treatment of single-unit data (left column) and of EMG records (right column). The discharge of one or a few motor axons recorded by 1 of up to 12 "hatpin" microelectrodes implanted chronically in the $L_5$ VR (18) was amplified ~7,000-fold and recorded on FM tape. Each microelectrode recording was played back from magnetic tape, filtered (1–10 kHz bandpass), and one or more single units were separated on the basis of spike amplitude and shape, using two window discriminators in tandem. Each occurrence of a discriminated spike caused the generation of a brief acceptance pulse, which was registered by the computer (Digital PDP 11/23). The time of occurrence of an acceptance pulse was measured to the nearest millisecond. An oscillographic hard copy (5-kHz bandpass; Honeywell Visicorder 1058) of the raw microelectrode recording and associated train of discriminator acceptance pulses provided visual confirmation of the accuracy of spike acceptance. When necessary, the computer data files were later edited in two ways: falsely accepted events were deleted and spikes that had missed being accepted by the window discriminators (because of coincidence with a spike from another unit or with noise or because of fluctuations in amplitude) were added. In the data files used in this study, <5% of all spikes required editing. The requirement for editing was usually greatest for faster treadmill speeds because the average unitary firing rates increased and additional, previously silent, higher-threshold units were recruited. Both events contributed to an increased chance of spike shape distortion through superposition. Recordings at higher treadmill speeds than those shown here were often available, but were not used for this study because the uncertainity in correcting for spike acceptance errors became unacceptably high.

### *Computation of the instantaneous unit "frequencygram"*

Each spike in a burst was assigned a value of instantaneous frequency equal to the inverse of the time interval since the occurrence of the previous spike. The frequency of the first spike in a burst reflected the time elapsed since the occurrence of the last spike in the previous burst. Since data files were started between bursts of activity of the motoneuron of interest, the frequency of the first spike in a file was defined, arbitrarily, as the inverse of the time elapsed since the file was started. In this study, the instantaneous frequency of first spikes was not analyzed. Only their time of occurrence mattered.

### *Treatment of initial doublets*

Four of the 51 motoneurons that comprised this study exhibited initial doublets in occasional steps (units I11B22, L2A33, MSU10, and Q4A8). We considered an initial doublet to have occurred when the interval between the first and second spikes in a burst was <20 ms and the interval between the second and third spike was longer. For the purpose of analyzing the scaling between the frequencygram and the EMG profile we edited out the second spike of initial doublets. In such cases we always displayed the scaled frequencygram both with and without second spikes (see Fig. 11). Deleting second spikes caused a slight reduction in the computed instantaneous frequency value of third spikes. Later spikes in a burst were not affected.

### *Computer processing of EMG data*

For the purpose of analysis, the EMG signals were retrieved from magnetic tape and played through pulsed sample-and-hold integrators (similar to Bak Electronics PSI-1). In a few cases (6 units) some of the EMG records had to be filtered further (200 or 500 Hz, high pass) prior to integration to eliminate movement-related artifacts. The pulsed integrators were externally triggered every 4 ms and produced accurate area-under-the-curve measures of EMG, which were read by the computer. The 4-ms intervals were synchronized by the originally recorded time code signal so as to guarantee that sampling intervals were repeatable despite any fluctuations in tape speed or starting point.

A typical file stored in the computer consisted of 16 s of data obtained during walking on a belt moving at a constant speed. Since cats sometimes advanced in spurts and thus the stepping rate could vary, we verified the regularity of walking from simultaneously videotaped records. A data file consisted of the times of occurrence of all spike acceptance pulses and the values of EMG amplitude for 4,000 consecutive samples taken at 4-ms intervals.

### *Mathematical fitting of unitary frequencygrams to EMG profiles*

For the purposes of numerical analysis and visual display, the data were digitally processed as follows (see Fig. 1). The EMG files were digitally smoothed (15-point moving average) to eliminate high-frequency components while still preserving features with frequency components of up to ~33 Hz. The smoothed EMG profile was then computer fitted to the points representing the unit's frequencygram, according to the simple multiplicative relation

$$F(t) = K \times E(t) \quad \text{for} \quad F > 0 \qquad (1)$$

where $F(t)$ is the instantaneous frequency of motoneuron discharge, $t$ is the set of occurrence times of spikes, and $E(t)$ the value of the smoothed EMG profile at such times. $K$, the scaling constant, was adjusted to minimize the mean squared difference between the points and the scaled EMG profile value at the times of occurrence of spikes. In preliminary work (39) we investigated the advantages

of including the unit's threshold of recruitment as an additive constant $T$

$$F(t) = K \times (E(t) - T) \quad \text{for} \quad F > 0 \qquad (2)$$

but we found that, in general, the simpler relation of *Eq. 1* gave a fit of equivalent quality (see Fig. 3, *B* and *C*). We therefore used *Eq. 1* for the bulk of the analysis presented in this paper.

We evaluated the quality of the fit from the coefficient of determination, $r^2$ (where $r$ = correlation coefficient). This gave the fraction of the total variance in motoneuron discharge that could be accounted for by fluctuations in the EMG profile. For each motoneuron, we superimposed a plot of $r^2$ given by each muscle, with the plot of motor-unit potential amplitudes recorded in each muscle (see Fig. 4). This provided a visual comparison of the agreement between *1*) target muscle identification using spike-triggered averaging and *2*) correlation between the frequencygram of a motor unit and the EMG profiles of each of the anterior thigh muscles.

In pilot trials, we also considered whether the smoothed EMG waveform should be translated back in time, to account for conduction delays in axonal spike propagation and action potential propagation along the muscle fibers. We tested the effect of translating the EMG waveform 5–10 ms back in time, to line up the occurrence of the ventral root spike with the peak of the corresponding muscle unit potential (see, e.g., Ref. 18, Fig. 5*B*). We used the equation

$$F(t) = K \times E(t + C) \quad \text{for} \quad F > 0 \qquad (3)$$

where the conduction delay C varied between 5 and 10 ms.

Since *Eqs. 1* and *3* gave fits of comparable quality, we used *Eq. 1* for the rest of the analysis.

### *Determination of motoneuron threshold for a treadmill speed of 0.5 m/s*

The threshold of recruitment of a motoneuron was defined as the instantaneous value of the digitally filtered EMG at the time when the first spike in a burst occurred, normalized with respect to the peak EMG. Average threshold values were computed from 16-s data epochs of constant-speed walking as described in the previous paper (18). For most units (20/32) we recorded useable data at a belt speed close to 0.5 m/s (±0.05 m/s), as well as at two or more additional belt speeds. We then calculated the threshold value corresponding to 0.5 m/s [called T(0.5)] by interpolation (see Fig. 6*C*, Ref. 18). For 9/32 units, we could only obtain useable data at speeds either below 0.45 m/s or above 0.55 m/s, but since we had data for at least three belt speeds we linearly extrapolated the computed thresholds to estimate T(0.5). For the remaining 3/32 units we were not able to estimate T(0.5) from the available data.

### *Intracellular stimulation*

Lumbar motoneurons were impaled with glass pipette microelectrodes in cats anesthetized with intravenous pentobarbital. The target muscle was determined from the antidromic responses elicited by electrical stimulation of the cut muscle nerves. Motoneurons were depolarized with current injection delivered through the bridge of the electrometer. The current waveform was generated by computer to replicate the smoothed EMG profile recorded previously from a walking cat. We adjusted by hand the amplitude and DC offset of the input current waveform, monitored membrane potential, and processed the resulting trains of action potentials through a window discriminator and an interspike-interval converter (similar to Bak ISI-1) to obtain the instantaneous frequencygram. We then adjusted the current until the resulting firing patterns of the impaled motoneuron best matched the firing patterns recorded during walking from a motoneuron that had projected to the muscle chosen as current template.

## RESULTS

### *Sample size*

Discharge patterns during locomotion were analyzed for 51 $L_5$ VR motoneurons that were shown, using the technique of spike-triggered averaging (18), to project along the femoral nerve and thus innervate one of the anterior thigh muscles. For 43 of these motoneurons, the muscle of destination was also identified by spike-triggered averaging onto EMG electrodes, allowing a determination of recruitment threshold and correlations between single-unit discharge and the activation pattern of the target muscle. Thirty-two motoneurons for which data of sufficient quality were available at several treadmill speeds were studied in the greatest detail using the computer fitting approach. This sample included two motor units that were recorded directly from the SAm muscle EMG in *cat M* on *days 3* and *10*. The potentials recorded from these motor units were sufficiently large and characteristic to allow clean discrimination from the background EMG. The observations reported here are based on the 32 units analyzed using the computer fitting approach. However, another 19 motoneurons that projected to the anterior thigh and over 100 other discriminated $L_5$ VR units, probably motoneurons projecting to trunk or hip muscles, showed the same general features in their discharge patterns.

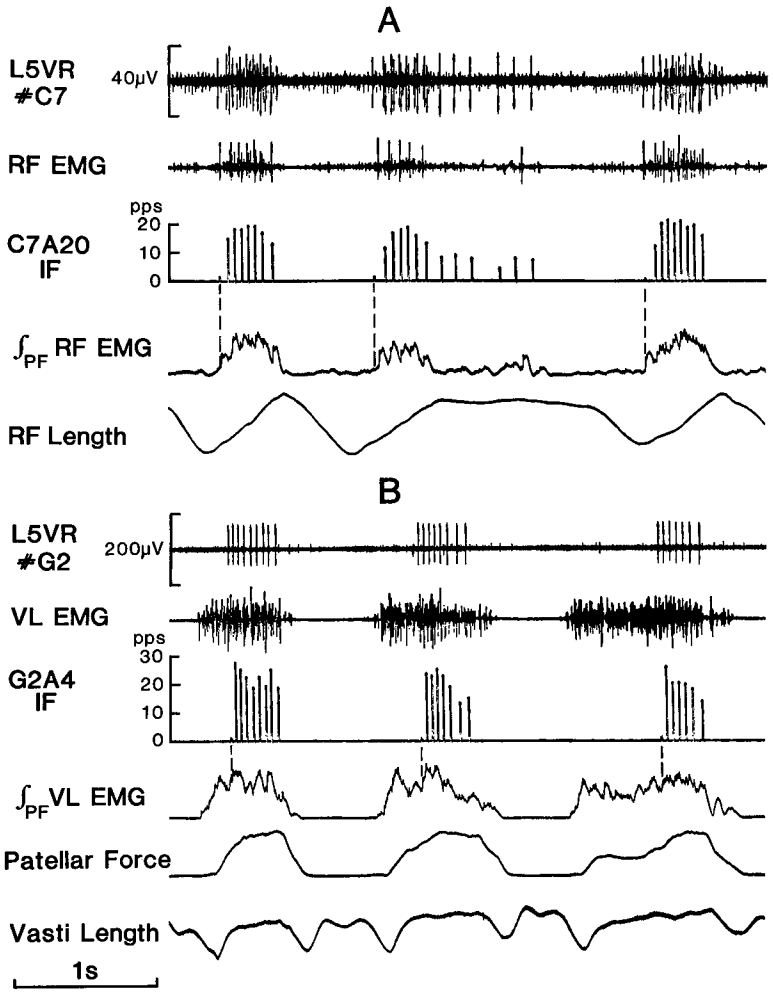


FIG. 2. *A*: example of natural activity patterns of a low-threshold RF motoneuron, C7A20, during locomotion at 0.2 m/s. *Top trace*: raw activity recorded in *cat C* on *day 20* by $L_5$ VR hatpin microelectrode no. 7. The largest spikes were produced by unit C7A20. *Second trace*: raw electromyogram recorded from RF, the target muscle for this unit. *Third trace*: instantaneous frequencygram computed for unit C7A20. Note the low instantaneous frequency that corresponds to the first spike of each burst (see METHODS). *Fourth trace*: rectified Paynter-filtered electromyogram (18) from RF. *Dashed vertical lines* indicate the time of occurrence of the first spike in each burst and intersect the filtered EMG profile at the threshold value for that step. *Last trace*: length gauge record corresponding to the RF muscle (lengthening upward). *B*: example of natural activity patterns of a high-threshold VL motoneuron, G2A4, during locomotion at 0.12 m/s. *Traces* as in *A*, except that VL is the appropriate target muscle for this unit. A patellar force gauge record is also shown. The *last trace* corresponds to the length of the vasti. See text for definitions.

### *Recruitment properties of single motoneurons*

At any given speed of walking, we invariably found that individual anterior thigh motoneurons *1*) were reliably recruited when the target muscle EMG approached a reproducible level (18) and *2*) when active, discharged a single burst of action potentials per step cycle. These findings applied to RF and sartorius motoneurons as well, even though the SA-a EMG consisted of two bursts of activity per step cycle (one during the stance phase and one during the swing phase) and a similar pattern was sometimes seen in RF for faster gaits. Other specific aspects of motoneuron recruitment that pertained only to sartorius and suggested a partition of functional roles in this anatomically complex muscle are addressed in the following paper (19).

*Modulation of the firing rate of motoneurons during locomotion*

Anterior thigh motoneurons showed marked modulation in their firing rates within a burst as well as from step to step. The examples in Fig. 2 show typical activation patterns for two motoneurons: a low-threshold motoneuron that innervated the RF muscle in *cat C* (unit C7A20; CV = 66 ± 7 m/s) and a higher-threshold motoneuron that innervated the VL muscle in *cat G* (unit G2A4; CV = 87 ± 9 m/s).

Motoneuron C7A20 was reliably recruited early in the development of each burst of RF EMG as the cat walked at 0.2 m/s (Fig. 2*A*). At this slow speed, the RF EMG record appeared to consist of relatively few motor units. The instantaneous frequency of motoneuron C7A20 was low at the beginning of each burst and thereafter increased roughly in parallel with the increasing EMG in its target muscle. Motoneuron firing rates as well as EMG amplitudes peaked midway through each burst and declined toward the end of each burst. This unit typically fired its last spike of each burst as the EMG was declining and was about to cross a level equivalent to the threshold for recruitment. In this sense, the threshold for de-recruitment of this motoneuron was roughly similar to its threshold for recruitment. The modulations in motoneuron firing continued to parallel the profile of the RF EMG even during the unusual protracted second step shown in Fig. 2*A*.

Motoneuron G2A4 was reliably recruited when the VL EMG reached ~85% of its peak value during slow walking at 0.12 m/s (Fig. 2*B*). The instantaneous frequency of this motoneuron was typically highest early in its recruitment. From then on its firing rate declined progressively, showing modulations that resembled the features of the smoothed VL EMG. Notably, motoneuron G2A4 persisted firing long after the EMG in its target muscle had declined below the recruitment threshold value. As a consequence, and in contrast to unit C7A20, G2A4 had markedly different thresholds of recruitment and de-recruitment. This was a consistent finding for all five high-threshold [T(0.5) > 70% of the peak target muscle EMG at 0.5 m/s] motoneurons encountered, all of which innervated either the vasti or RF. Additional examples of high-threshold motoneurons are shown in Fig. 5 (unit M11A10) and Fig. 8 (unit L7A29).

*Computed correlations between the unitary frequencygram and the EMG profile of its target muscle*

The instantaneous frequencygrams of 32 motoneurons were computer fit to the rectified smoothed EMG of each of the anterior thigh muscles by multiplying the amplitude of the EMG waveform by a suitable scaling factor $K$ (see *Eq. 1*). A general finding using this approach was that the frequencygram of a single motoneuron was more closely correlated to the smoothed EMG of its target muscle than to the EMG of any other anterior thigh muscle. As shown below, a simple multiplicative function of the target muscle EMG profile typically accounted for most of the variance (0.88–0.96) in the frequencygram of a motoneuron during locomotion, a property that persisted for all speeds of locomotion investigated.

A representative example is shown in Fig. 3. Motoneuron M11A8, active during the stance phase, was found to innervate the RF muscle on the basis of spike-triggered averaging. A plot (described in Ref. 18) that compares the amplitude of the motor-unit potentials recorded in each muscle is shown in Fig. 4 (solid lines). The unit frequencygram was fit to the EMG profiles of the five relevant anterior thigh muscles (see METHODS, Fig. 1). Visual inspection of Fig. 3 suggests that the closest fit was provided by the RF muscle EMG profile, at least for the four steps shown. The frequencygram for unit M11A8 tended to peak late in each step and the RF EMG profile matched this shape closely, whereas the vasti tended to peak earlier in each burst and turn off more gradually. SA-a had stance-phase EMG bursts of considerably different shape, with dual peaks early and late in each burst, and consequently provided a poor visual fit. Computation of the best mathematical fit for each muscle, based on 16 s of data comprising 14 steps at a walking speed of 0.37 m/s, showed that the RF EMG profile accounted for 0.90 of the variance in the instantaneous frequency of this motoneuron. Best fits using the other muscles could account only for 0.67–0.84 of the variance. This finding was reproduced at two other available treadmill speeds, 0.14 and 0.25 m/s. Two factors seemed to account for

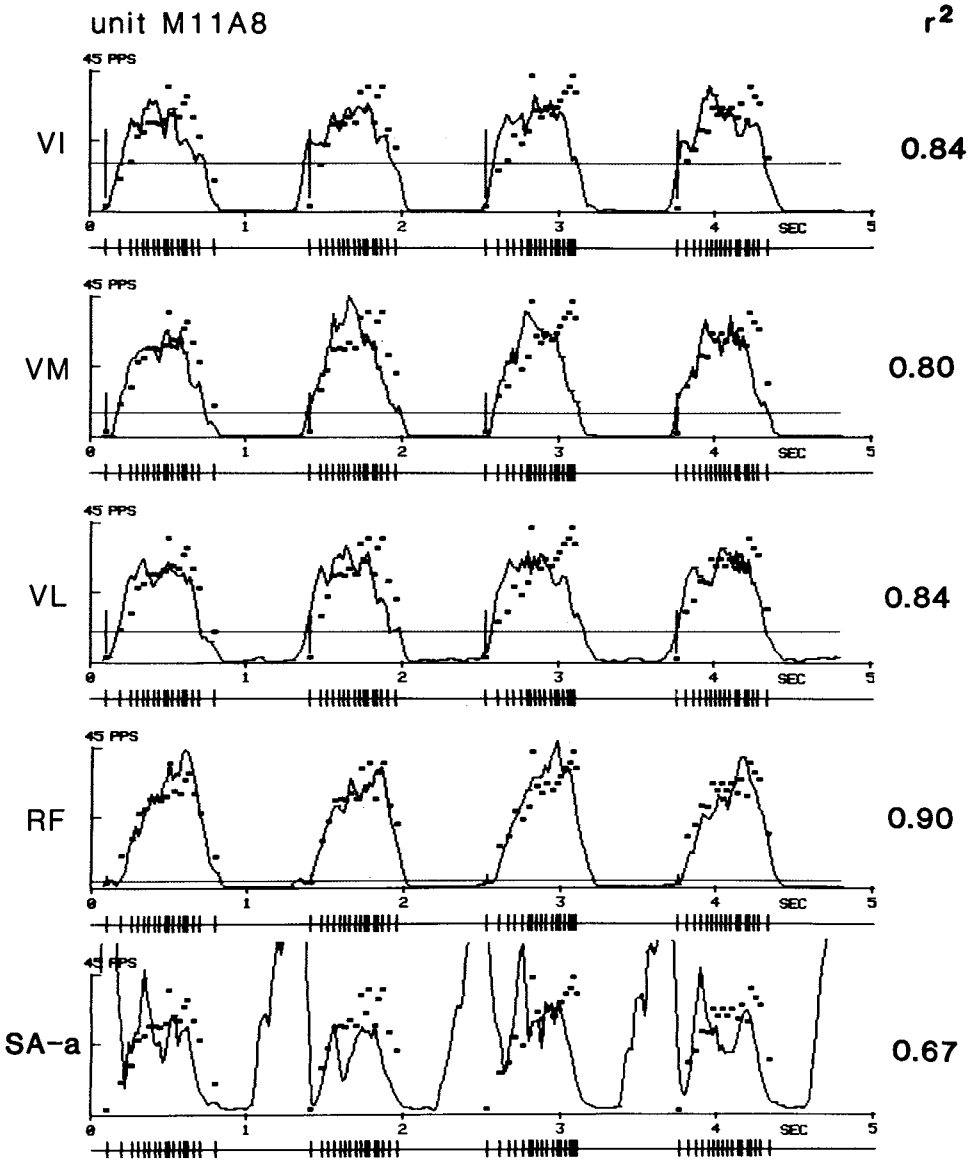


FIG. 3. Examples of computer-fitting the frequencygram of a $L_5$ VR motoneuron, M11A8 to the filtered EMG profile of each of the 5 extensor muscles of the anterior thigh. The same 5-s segment (part of a 16-s data epoch obtained during walking at 0.37 m/s) was fitted to the EMG of a different muscle in consecutive panels. The fraction of the total variance in unit frequency that was accounted for by each EMG profile is shown at *right*. The RF EMG provided the best fit. Through the use of spike-triggered averaging, RF was also shown to be the target muscle of motoneuron M11A8 (see Fig. 4). See text for definitions.

the tightness of the RF correlation: first, the overall shape of the typical RF burst was closest to the shape of the motoneuron burst; second, step-by-step variations in amplitude as well as higher-frequency fluctuations in the RF EMG envelope best reflected the M11A8 motoneuron activity.

### *Relationship between motoneuron frequencygram fits and the results of spike-triggered averaging*

To test how consistently the frequencygram of a motoneuron was best fit by the EMG profile of the "target muscle" identified with spike-triggered averaging, we compared the two plots

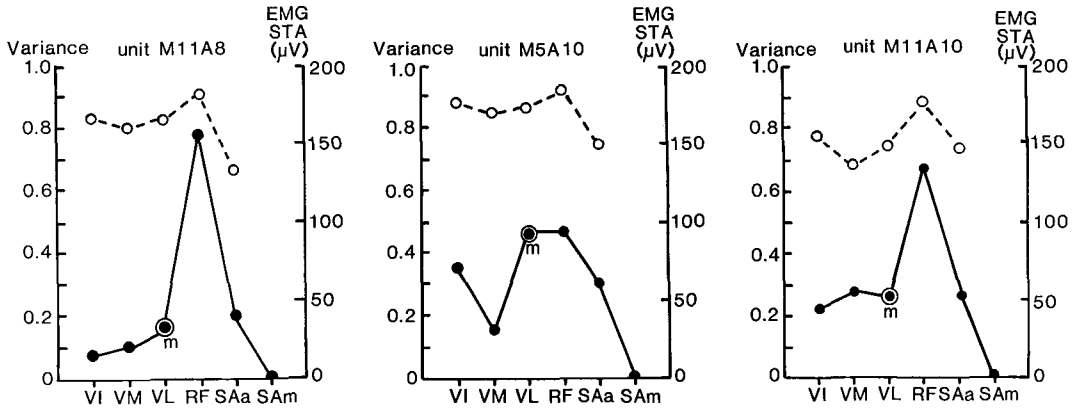


FIG. 4. Superimposed amplitude plots for 3 motoneurons recorded from the same cat. *Filled circles* joined by *solid lines* show the amplitude of the motor-unit potential recorded by EMG electrodes in each of the 6 anterior thigh muscles, computed with spike-triggered averaging (1,024 sweeps). Actual voltage calibrations are shown along the *right ordinates* (EMG STA). The VL potential amplitudes were unusually large because the EMG electrode was monopolar (m). All 3 motoneurons innervated the RF muscle. *Open circles* joined by *dashed lines* show the fraction of the variance in motoneuron firing frequency accounted for by the rectified smoothed EMG profile of each anterior thigh muscle active during the stance phase of locomotion. Calibrations are shown along the *left ordinates.* Plot for unit M11A8 derives from data shown in Fig. 3. All 3 motoneurons were best fitted by the RF EMG profile. See text for definitions.

for 32 motoneurons that were analyzed by both methods. Examples for three units (M11A8, M5A10, M11A10) presumed to project to the same muscle (RF) are shown in Fig. 4. These units were recorded from the same cat within a 3-day period, so the configuration of the implanted EMG electrodes was the same. The motor-unit potential amplitudes obtained with spike-triggered averaging are plotted as filled circles joined by solid lines, with calibrations shown along the right ordinates. For two motoneurons, M11A8 and M11A10, the plots that resulted from spike-triggered averaging suggested quite unambiguously that RF was the target muscle. For unit M5A10 the potentials recorded by RF and VL were of similar amplitude and the VI and SA-a potentials were not much smaller. However, one of the VL EMG electrode wires had broken, forcing the "monopolar" recording of the VL EMG to be referred to a distant ground. Spike-triggered averaged "monopolar" potentials could often be of large amplitude even when the motor unit actually resided in another muscle, but they usually consisted of somewhat lower-frequency components. This information, plus the lower frequencies contained in the smaller VI and SA-a potentials, suggested that RF was also the target muscle of motoneuron M5A10.

### *Confirmation of target muscle from best fits*

For all three units shown in Fig. 4, the best fit was provided by RF, the same muscle identified by spike-triggered averaging. We found, in general, that the "target muscle" of a motoneuron determined by spike-triggered averaging (an "anatomical" property deriving from the morphological localization of the motor unit within the anterior thigh muscle group) was also the muscle that generated EMG bursts that reflected most closely the activation characteristics of the motoneuron (a "physiological" property). For 18 knee extensor motoneurons in the sample of 26 (69%), the two methods, spike-triggered averaging and variance estimation, resulted in the same choice of target muscle. For another 4/26 motoneurons (15.5%) the choice of target muscle suggested by spike-triggered averaging was the second choice based on variance estimation, or vice-versa. For only 4/26 motoneurons (15.5%) the results of spike-triggered averaging and variance estimation did not agree. However, in three of these four cases, one or several of the EMG electrodes had become monopolar. In such cases we found that the computer fits gave less ambiguous results.

Interestingly, two of the motoneurons in Fig. 4 had low thresholds of recruitment

(M11A8, 3%; M5A10, 9%) and the third motoneuron had a higher threshold (M11A10, 85%). The threshold value did not have any influence on the generality of the finding of high correlation between the identification of target muscle based on spike-triggered averaging and on frequencygram fits.

*General relationship of motoneuron firing to target muscle EMG*

Typical discharge patterns characteristic of high- and low-threshold motoneurons are shown in Fig. 5, for the two RF units recorded simultaneously (M5A10 and M11A10) as *cat M* walked uniformly at a belt speed of 0.48 m/s. In Fig. 5*A*, the amplitude of the smoothed RF EMG was scaled to fit the frequencygram of each motoneuron, by choosing the value of $K$ that minimized the summed square of the distance from the frequencygram dots to the EMG profile. The best fits were calculated from 16 s of data that included the 5 s of data shown in Fig. 5*A*. By coincidence, the value of $K$ was the same ($K = 0.031$) to optimally fit the frequencygrams of the two motoneurons, in spite of marked differences in their thresholds and in the total number of spikes fired per step.

Figure 5*A* exemplifies features shared by all 32 motoneurons analyzed by the fitting approach. First, each motoneuron was reliably recruited as the EMG profile of its target muscle reached a reproducible value. Motoneuron M5A10 had a low threshold for recruitment, of the order of 9 ± 7% (SD) of the average value of peak EMG reached by the RF muscle at this speed of walking. A vertical line, drawn at each time of recruitment of the motoneuron, intersected the EMG profile at the threshold EMG value for that step. The length of the vertical line indicates ±1 SD about the mean threshold value for all steps taken during that 16-s epoch. The mean threshold is displayed in Fig. 5*A* as a thin horizontal line. M5A10, a low-threshold motoneuron, was recruited early in each RF EMG burst and fired trains of action potentials that lasted almost as long as the EMG burst itself. In Fig. 5A, unit M5A10 fired 12, 12, 10, 12, 12, and 14 spikes during the six bursts. The peak frequency of firing was 30–35 spikes/s during each of these steps. Step by step, the frequencygram was modulated in a characteristic manner that generally resembled the shape of the corresponding RF EMG bursts.

In contrast, motoneuron M11A10 (bottom panel of Fig. 5*A*) had a high threshold for recruitment. It was recruited when the RF EMG reached 73 ± 12% of its average peak EMG value for this speed of walking. This meant that M11A10 was active during a relatively brief portion of each step, mainly during the second half of the activity burst of the RF muscle. During the steps shown in Fig. 5*A*, motoneuron M11A10 fired 6, 7, 6, 5, 6, and 6 spikes, respectively. However, its peak frequency of discharge was comparable to the lower-threshold motoneuron M5A10 for the same steps.

A comparison of the frequencygrams of the two motoneurons indicated that the low-threshold unit, M5A10, tended to reach a rounded plateau midway through the activity period. The peak firing frequency attained for each step varied less than the peak RF EMG and occurred as, or slightly before, the RF muscle EMG reached its peak for each step. The high-threshold unit M11A10, in contrast, fired sharper bursts that only peaked late in each step, later than the RF muscle EMG, although the peak frequencies appeared to match closely the amplitude of the RF EMG peaks attained in individual steps.

The differences in the shapes of frequencygrams of high- and low-threshold motoneurons prompted us to test whether frequencygrams might be better fitted by the *net portion* of the smoothed EMG of the target muscle. This meant subtracting a constant value, the threshold of the unit, from the EMG profile (see *Eq. 2*). Examples of fitting the net RF EMG to the frequencygrams of the same two motoneurons are shown in Fig. 5*B*, for two steps taken at a speed of 0.14 m/s. In the bottom trace of Fig. 5*B*, the thresholds of the two units are superimposed onto the full RF EMG profile. In practice, for low-threshold motoneurons, the approach of *Eq. 2* did not represent a major change from the simpler fit of *Eq. 1*, because only a small DC component was subtracted. In contrast, for high-threshold motoneurons it could represent a potentially important change because only the shape of the "tip" of the EMG profile was used for the fit. However, in pilot trials the goodness of fit turned out to be roughly comparable using *Eqs. 1* or *2*. This finding may have been due

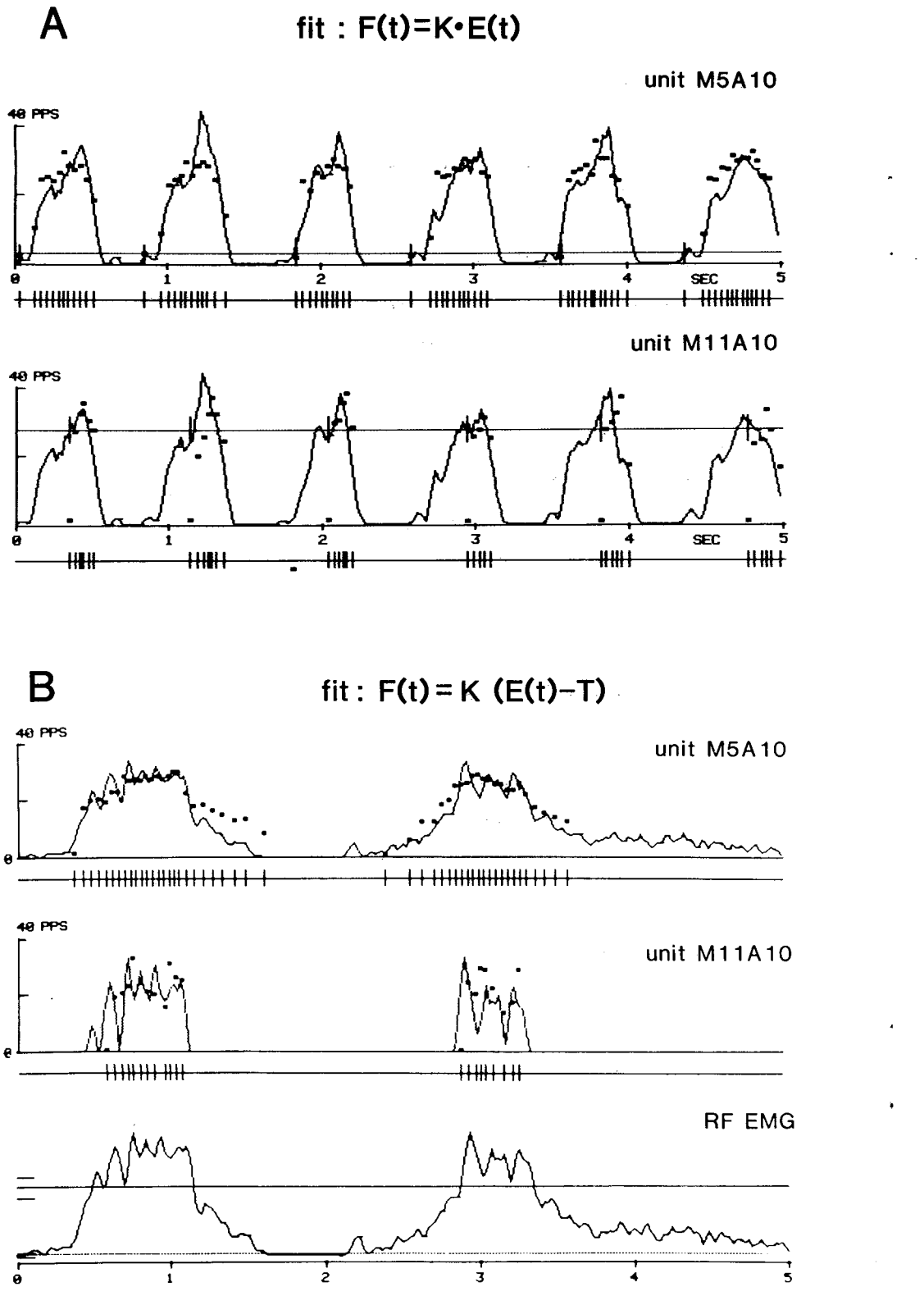
A
fit : F(t)=K•E(t)
unit M5A10
40 PPS
0
1
2
3
4
SEC
5
unit M11A10
40 PPS
0
1
2
3
4
SEC
5
B
fit : F(t) = K (E(t)–T)
40 PPS
unit M5A10
0
40 PPS
unit M11A10
0
RF EMG
0
1
2
3
4
5

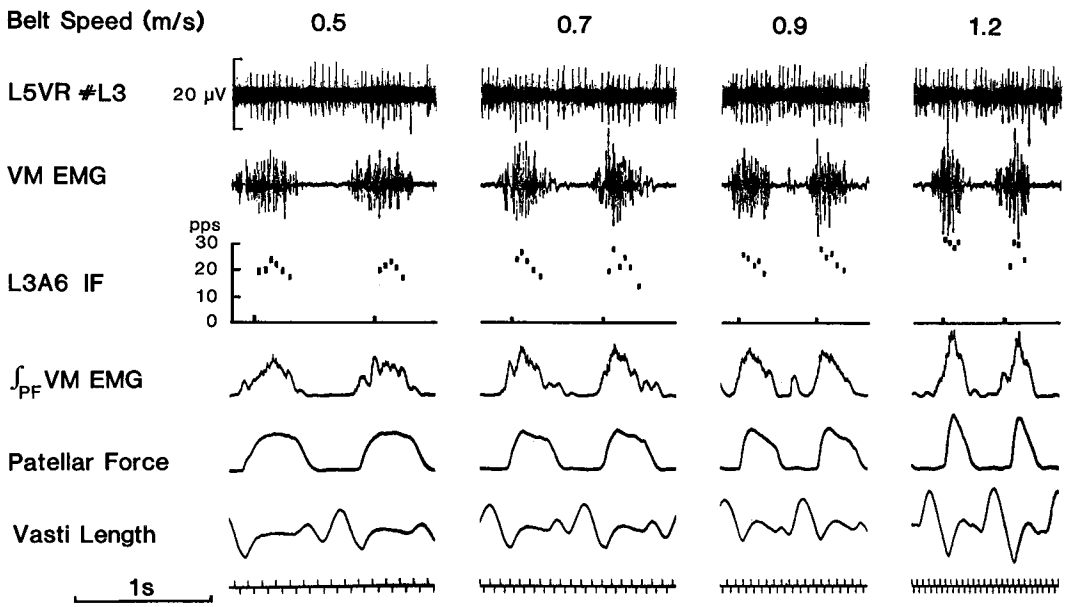


FIG. 6. Activity of a VM motoneuron as a function of speed of locomotion. The raw microelectrode record contained spikes generated by two units, but the motoneuron of interest was cleanly discriminated on the basis of spike shape. Four speeds are shown. *Traces* as in Fig. 2*B*. Both the mean and peak firing frequency tended to increase with increasing treadmill speed. See text for definitions.

to the magnified variance in the smoothed net EMG profile. For this reason, we used the simpler approach of *Eq. 1* for the 32 units reported here.

For the examples shown in Fig. 5*A*, the fractional variance accounted for by the RF EMG fit was 0.89 for unit M11A10 and 0.92 for unit M5A10 (see Fig. 4). When tested across the population of units recorded, no systematic differences were detected in the quality of fit obtained for high-, medium-, or low-threshold motoneurons using the whole target muscle EMG as template (*Eq. 1*).

### *Dependence of motoneuron discharge rates on the speed of locomotion*

A finding common to most recorded motoneurons was that their firing rates reached higher levels at faster treadmill speeds. An example is shown in Fig. 6, where the activity of a VM motoneuron [unit L3A6; CV = 117 m/s; T(0.5) = 60%] was recorded at four belt speeds ranging from 0.5 to 1.2 m/s. At the fastest speed the cat was trotting rather than walking, causing the larger excursions of the knee extensor muscles (vasti length trace). The two steps shown for each speed are representative of continuous recordings obtained as the cat stepped steadily for at least 30 s at each speed. For increasing speeds, the following features emerged: *1*) the amplitudes of the Paynter-filtered VM EMG (18) and the patellar force increased; *2*) both the average and peak frequency of discharge of the discriminated motoneuron, L3A6, increased; *3*) the duration of VM EMG and patellar force decreased; *4*) the duration of the motoneuron bursts decreased, and *5*) the number of motoneuron spikes per burst decreased. In ad-

FIG. 5. Computer fits for a low-threshold RF motoneuron, M5A10 and a simultaneously recorded high-threshold RF motoneuron, M11A10. *A*: result from using *Eq. 1*, where the full EMG profile was fitted to the frequencygrams. The mean threshold for each motoneuron is indicated by a *horizontal line* and the standard deviation of the threshold is indicated by *vertical segments* at the times of occurrence of the first spike in each burst. Treadmill speed in *A*: 0.48 m/s. *B*: result from using *Eq. 2*, where the magnitude of the corresponding threshold was subtracted from the RF EMG before fitting each frequencygram. The two motoneurons are the same as in *A* but the data epoch is different. The *bottom panel* shows the RF EMG and the average thresholds (±1 SD shown at *left*) for the two units. Treadmill speed in *B*: 0.14 m/s. Further description in text.

dition, it can be seen that the motoneuron attained its peak frequency during each burst at approximately the same time as the VM EMG reached its maximum value for that step.

Figure 7*A* shows that the speed-dependent discharge behavior observed for unit L3A6 was a general finding. Figure 7*A* shows the behavior of the seven motoneurons that were recorded from *cat L* for several belt speeds. (An 8th motoneuron, unit L2A33, was excluded from this analysis because it exhibited occasional high-frequency initial doublets; see below.) To obtain the data points in Fig. 7*A*, the peak values of firing frequency during each motoneuron activity burst were averaged for all the bursts that occurred during the 16-s data stretch analyzed for each speed of locomotion. (Curves of nearly identical shape were obtained by averaging mean firing frequencies, rather than peak values; not shown.) For all motoneurons, the peak (and mean) firing frequencies tended to increase with treadmill speed. There were only three exceptions to a strict monotonic upward trend for all units at all speeds: motoneurons L3A4 and L4A4 on *day 4*, and motoneuron L4A14 on *day 14*. In those three cases, the motoneurons had reached unusually low discharge frequencies at the second lowest of the walking speeds tested (indicated by arrows in Fig. 7*A*), when compared with the lowest speeds tested.

Interestingly, for the three unusual cases the rectified and smoothed EMG of the corresponding target muscles had also reached lower peak values at the second speed than at the slowest speed of walking. An example is

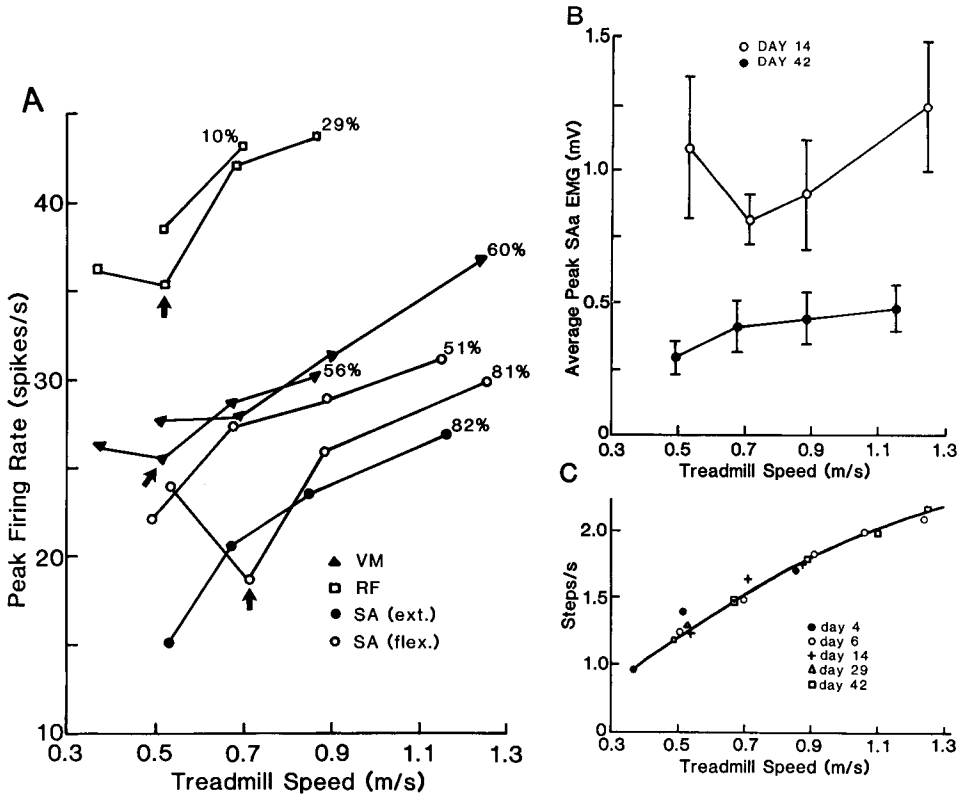


FIG. 7. *A*: relationship between peak firing rate and treadmill speed, shown for 7 motoneurons recorded in *cat L*. The recruitment threshold [T(0.5)] is indicated for each unit. *Symbols* indicate the target muscle of each unit (see key). *Arrows* indicate exceptions to monotonically increasing trends (see text). *B*: comparison of the average peak EMG recorded from *cat L*, SA-a muscle, on *days 14* and *42*. *Error bars* indicate 1 SD *C*: relationship between stepping rate and treadmill speed, *cat L*, on five different days (see key). Most of the data were well fitted by a smooth curve. *Two points* that departed markedly from the curve correspond to *days 4* and *14*, when the exceptions in Fig. 7*A* took place. Further description in text.

given in Fig. 7*B*, where the average peak EMG values generated in SA-a on *day 14* and on *day 42* are displayed at comparable treadmill speeds. The disparity in the trends for the two lower speeds of walking in the 2 days suggested that, on *day 14, cat L* had somehow changed its muscle recruitment strategy when adjusting to a transition in treadmill belt speed. This hypothesis was confirmed by plotting the average stepping rates that *cat L* used during each 16-s data file from which Fig. 7*A* was compiled. The result is shown in Fig. 7*C*. On most days, ranging from *day 4* to *day 42* postimplant, *cat L* had increased its stepping rate gradually and progressively as the belt speed was increased; most of the data points in Fig. 7*C* were well fitted by a smooth curve. On two occasions, however, the cat stepped at a faster rate in response to the first transition in belt speed. The exceptions corresponded to *day 4* at 0.52 m/s and *day 14* at 0.71 m/s, which are exactly the occasions when unusually low motoneuron firing rates were observed in Fig. 7*A* and unusually low peak EMG was observed in the target muscle in Fig. 7*B*. The conclusion was that *cat L* had taken more frequent steps at those particular recording sessions. Of necessity, the amplitude of each step was reduced in order for the cat to maintain a constant forward speed on the moving belt. Consequently, the amplitude of EMG generated in the anterior thigh muscles was lower than average for that speed of walking, and the reduced level of drive was also reflected in the peak discharge rates of individual motoneurons. This example serves to demonstrate further the tightness of the relationship between the firing rates of individual motoneurons and the EMG levels of their target muscles. It also demonstrates the variety of parameters that define, and must be monitored to describe, motor behavior in an intact freely moving animal.

With due consideration of the exceptions in the data of Fig. 7*A*, we concluded that the firing rates of individual motoneurons generally increase monotonically for faster speeds of locomotion. The increase in firing rates can be considerable. The average slope in Fig. 7*A* indicates that cat anterior thigh motoneurons tend to increase their firing rate by ~10 spikes/s in order to increase walking speed by 0.6 m/s, in the range between 0.4 and 1.2 m/s. The relation between motoneuron discharge rate and treadmill speed is probably not linear: the firing frequencies of individual units probably tend to saturate for higher speeds, although we could not collect sufficient data at high speeds of locomotion to confirm this.

Additional details of the relationship between motoneuron firing and target muscle EMG profile at different speeds of locomotion emerged from the computer fitting strategy. The example shown in Fig. 8 was a high-threshold motoneuron, unit L7A29, which was fitted to the VM EMG profile at three belt speeds, 0.53, 0.68, and 1.16 m/s. This motoneuron was recruited when the VM muscle reached 83% of its peak value at the lowest speed of walking shown, 0.53 m/s. As can be seen in Fig. 8*A*, at 0.53 m/s this motoneuron was not reliably recruited; for one weaker step it did not reach threshold, and the VM EMG also did not reach the computed threshold level for this unit. For a 16-s epoch at the lowest speed of walking, unit L7A29 fired on average 1.9 spikes/step and reached an average peak frequency of 15.1 pps. When active, its instantaneous frequency was extremely well fitted by the VM EMG. The EMG profile accounted for 0.95 of the variance in the motoneuron firing rate.

At the somewhat faster walking speed shown in Fig. 8*B*, 0.68 m/s, unit L7A29 was consistently recruited for every step. It fired more spikes per step (2.8 on average) and reached higher peak frequencies (20.6 pps). The instantaneous frequency continued to match closely the shape of the VM EMG, which accounted now for 0.93 of the variance. The scaling factor increased somewhat, from $K = 0.041$ for the slower speed, to $K = 0.049$. This meant that the EMG profile had to be multiplied by a slightly larger number in order to keep up with the unit firing profile. Thus, if the peak EMG was increasing linearly with treadmill speed (see Fig. 7*B*), the firing frequency of this high-threshold motoneuron was increasing slightly more than the average VM motoneuron.

At the fastest recorded speed, unit L7A29 (then securely recruited; Fig. 8*C*) fired 3.6 spikes/step and reached a mean peak frequency of 26.9 pps. The VM EMG profile continued to match closely the variations in frequency in the unit and could predict 0.90 of the variance during 16 s of data. The standard deviation for the recruitment threshold

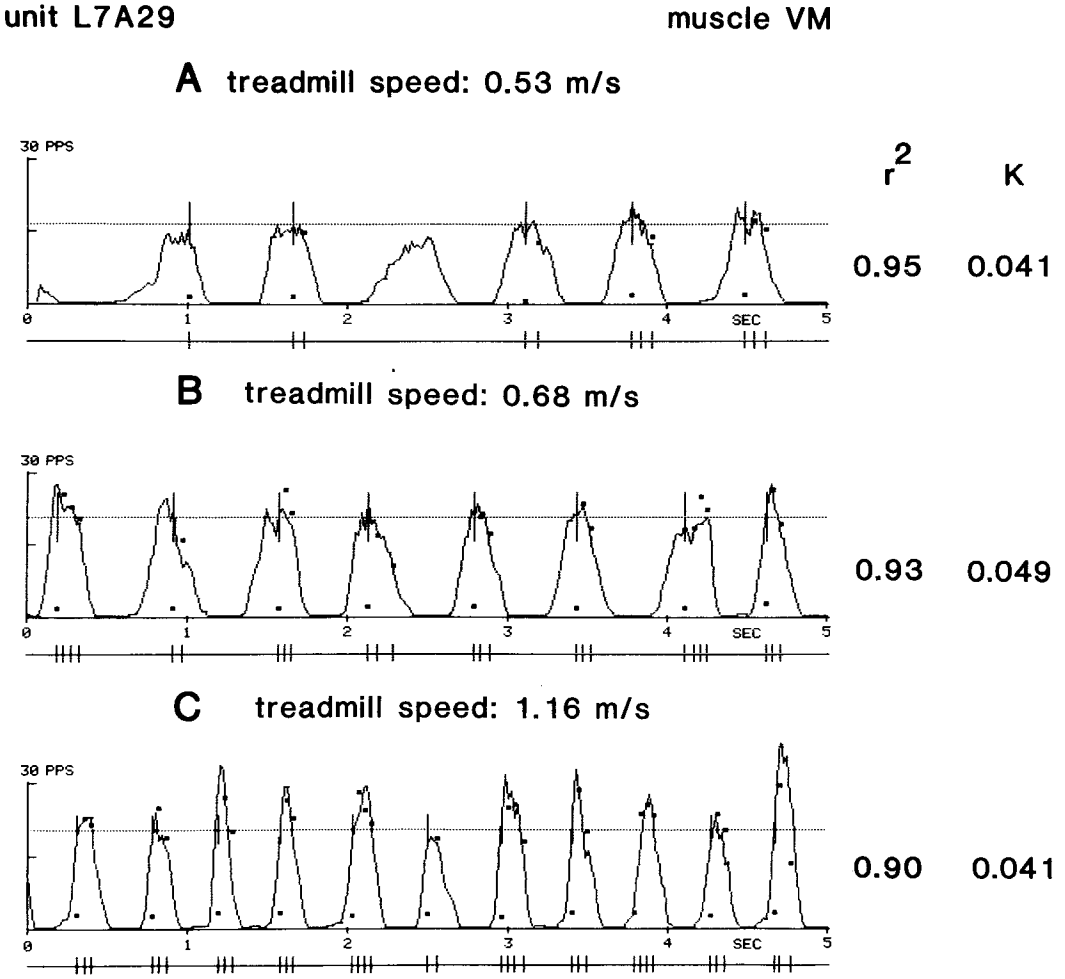


FIG. 8. Results of computer fitting the frequencygram of a high-threshold motoneuron (L7A29) for three speeds of locomotion. A *horizontal line* shows the computed average recruitment threshold for each speed. The fraction of the total variance ($r^2$) accounted for by the VM EMG profile and the computed scaling factor ($K$) are indicated for each speed.

(shown by the vertical bars) was actually smaller at the faster speed than at lower speeds of walking, once this motoneuron was being recruited securely. The step-by-step variations in unit frequency kept pace faithfully with variations in the VM EMG profile (e.g., the 6th and 11th steps in Fig. 8*C* had weaker and stronger EMG than average but the frequencygram remained tightly matched). The best fit was given by $K = 0.041$, the same as for the lowest speed of walking. For most motoneurons the scaling factor $K$ changed little over the whole range of belt speeds (see next section). These findings, taken together, suggested strongly that every recruited motoneuron was being driven by a synaptic input that was common to the entire pool of motoneurons and this common drive was accurately reflected in the multiunit EMG.

The high-threshold motoneuron L7A29 (Fig. 8) was somewhat atypical in that the number of spikes/burst increased with treadmill speed. Most motoneurons tended to fire fewer or the same number of spikes per burst at faster speeds of walking. Figure 9*A* shows trends for seven motoneurons recorded in *cat L*. Since both the peak and the average frequency of firing increased and fewer spikes

were fired per burst, motoneuron *burst durations* decreased markedly for faster treadmill speeds. This was consistent with decreased durations of EMG bursts at faster speeds in anterior thigh muscles active during the stance phase (see Figs. 6, 8; also Ref. 11).

*Dependence of scaling factor K on speed of locomotion*

The variation in $K$ as a function of speed is shown in Fig. 9*B* for 21 motoneurons. (A logarithmic ordinate was used to accommodate variations in the magnitude of $K$ that simply reflected the original EMG recording gains for the various target muscles.) Only for 2/21 units did $K$ vary by $>\pm 15\%$ over the range of speeds analyzed. For 3/21 units, $K$ increased somewhat for faster walking. For most units, 12/21, $K$ decreased modestly for increasing speeds. This observation was consistent with additional motor-unit recruitment resulting in faster growth of the target muscle EMG than

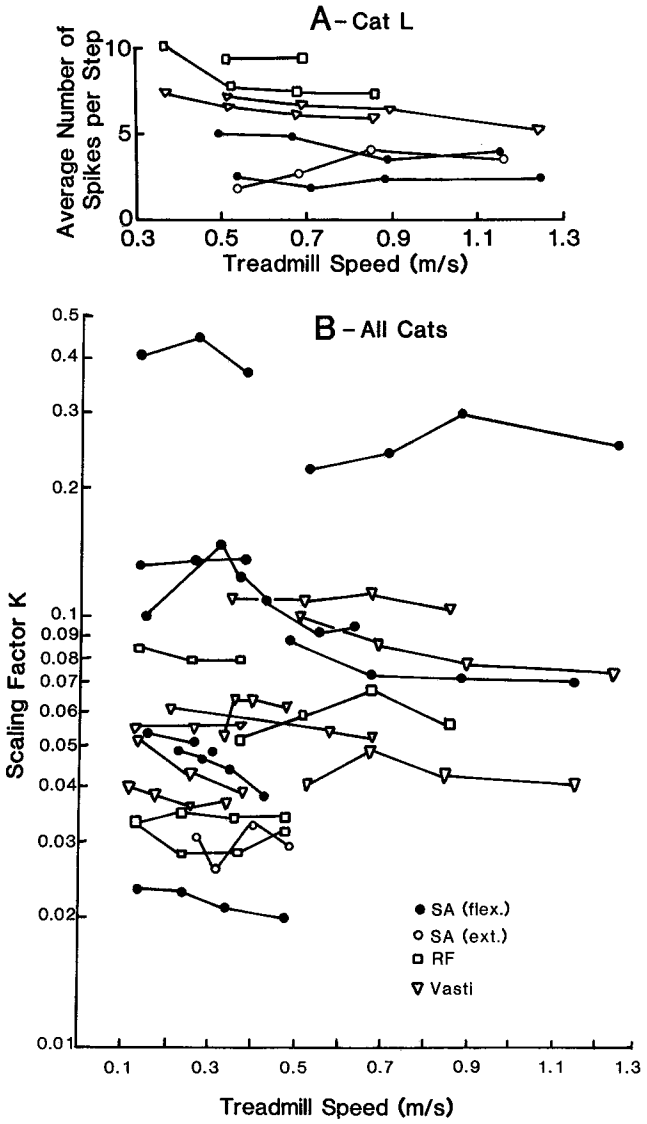


FIG. 9. *A*: relationship between average number of spikes per step and treadmill speed for 7 motoneurons recorded in *cat L*. *B*: relationship between scaling factor, $K$, and treadmill speed for 21 motoneurons recorded in different cats. Key to target muscles also applies to *A*. Note the logarithmic *ordinate*.

would occur with rate coding alone (see DISCUSSION).

*Relationship between firing rate and threshold of recruitment*

The data in Fig. 7*A* indicated that in *cat L*, low-threshold motoneurons usually reached higher peak frequencies than high-threshold motoneurons at matched speeds of locomotion. The generality of this finding is further documented in Fig. 10, where the average peak firing frequencies reached by 18 motoneurons at a belt speed of 0.5 ± 0.05 m/s are displayed against their T(0.5) values. Only one high-threshold RF motoneuron (M11A10) deviated from the trend by exhibiting high firing frequencies. The significance of this trend will be addressed in the DISCUSSION.

*Absence of initial doublets*

An unexpected finding was that, in contrast to locomotion in decerebrated cats (42), initial doublets at the beginning of bursts were seen very rarely in normal cat locomotion. Only four out of 51 anterior thigh motoneurons showed initial doublets at any time during locomotion. These units were: I11B22 [VI, CV = 57 m/s, T(0.5) = 32%]; L2A33 [VI, CV = 104 m/s, T(0.5) = 67%]; Q4A8 [VM, CV = 91 m/s; T(0.5) = 74%]; and MSU10 [SA-m, CV unknown, T(0.5) = 15%]. Three of the four units projected to VI or VM, the "red" muscles in the anterior thigh. The fourth unit was actually discriminated from the SA-m EMG record during walking. It was a low-threshold muscle unit with a large potential that was clearly visible in the raw EMG record and could be isolated cleanly. Since this was considered an important unit for further analysis, a special effort was made to obtain a reference EMG record from the target muscle, SA-m, that was not dominated by the motor unit under study. The large-amplitude brief-duration contributions by the unit were electronically clipped out of the EMG record using a Schmitt trigger and a clipper. In this way, a reasonable raw SA-m EMG signal was obtained that was considered representative of

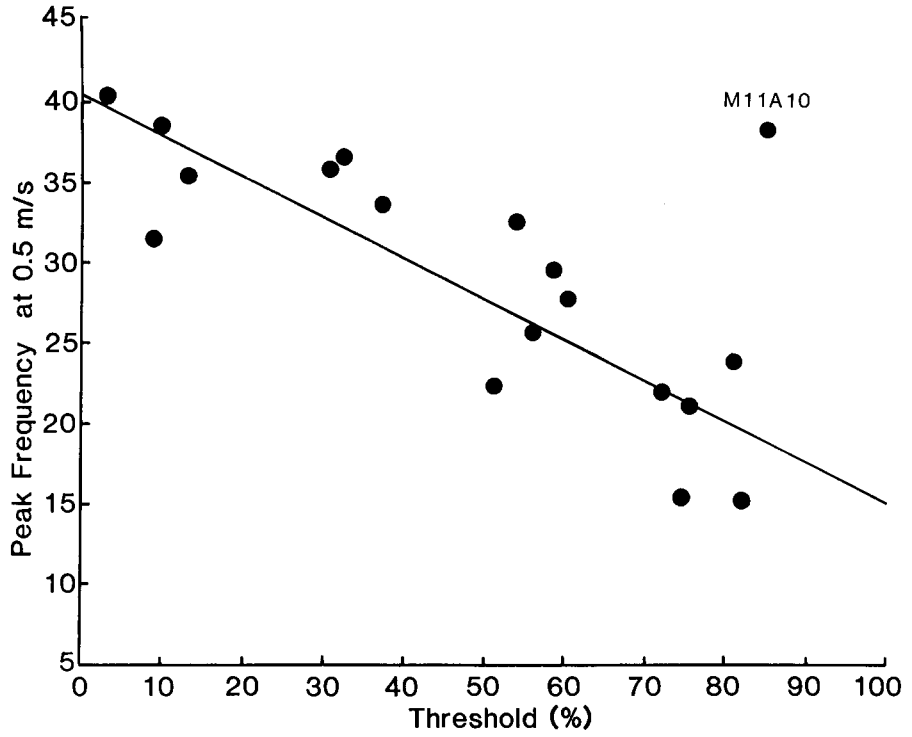


FIG. 10. Relationship between peak firing frequency (computed at a matched speed of 0.5 ± 0.05 m/s) and threshold of recruitment T (0.5) for 18 motoneurons. Only one (high-threshold) motoneuron, M11A10, departed from the trend shown by the fitted line.

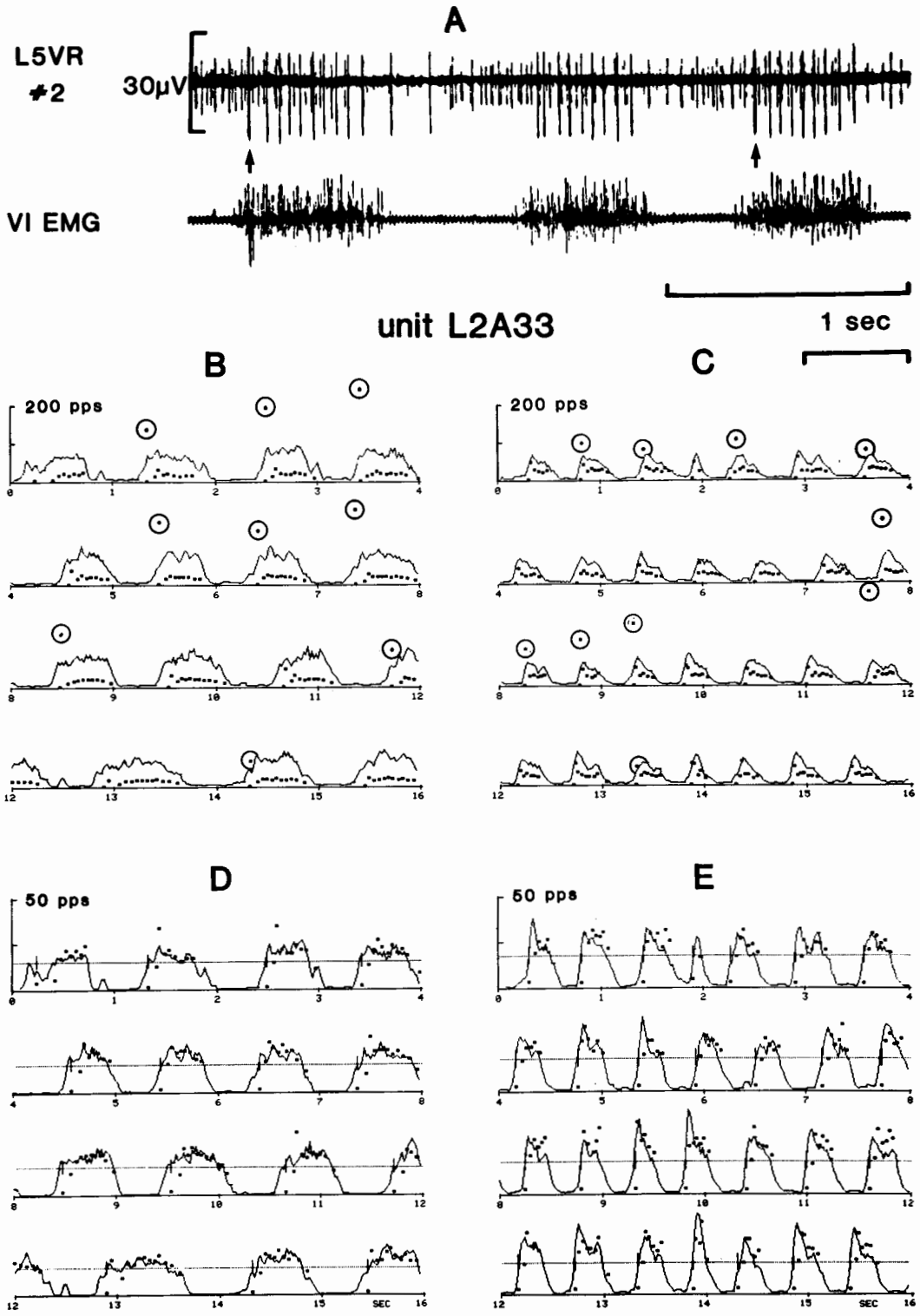


FIG. 11. Example of motoneuron that often fired initial doublets. *A*: raw records from microelectrode no. 2 in the $L_5$ VR. Largest spikes were produced by motoneuron L2A33. *Arrows* indicate the occurrence of initial doublets

the aggregate activity of the other units in the muscle. The clipped EMG signal was then processed in the usual way (Fig. 1, right column) to obtain a smooth profile of the target-muscle EMG. This allowed us to apply curve-fitting analysis to the discharge patterns of MSU10.

An example of a motoneuron that fired initial doublets, unit L2A33, is shown in Fig. 11*A*. The raw VR microelectrode and VI EMG records are shown for three steps taken at a belt speed of 0.32 m/s. Unit L2A33 produced the largest spikes visible in the upper trace. At this sweep speed, the occurrence of closely spaced doublets at the beginning of the first and third bursts is apparent only from the thickening of the trace (arrows). Following the occurrence of each doublet, the next interspike interval was considerably longer than average. This was consistent with observations in decerebrated cats (24, 42).

For unit L2A33, which we were able to record at several speeds, the probability of starting a burst with a doublet *decreased* for faster walking. The example in Fig. 11, *B* and *C* shows data collected while walking for 16 s at 0.32 and 0.85 m/s. The target muscle EMG is shown only for reference; with doublets present the vertical scales were not adjusted for best fit. The occurrence of initial doublets is signaled by the presence of second spikes with high frequency at some steps (circled data points). In Fig. 11*B*, high-frequency interspike intervals (>50/s) occurred in 9 out of 15 steps, or 60% of all steps. At the faster speed (Fig. 11*C*), high-frequency initial doublets occurred in only 9 out of 28 steps, or 32% of all steps. In addition, at the slower speed the average frequency of the initial doublets was 142 pps, whereas at the faster speed the average frequency of the initial doublets was only 118 pps. Thus both the incidence of initial doublets and their instantaneous frequency declined at the faster speed of walking.

In all four units that often fired initial doublets, the instantaneous frequency for the rest of the motoneuron burst still showed marked modulations that were closely correlated with the target muscle EMG profile. This was in contrast to data obtained previously from decerebrated cats (24, 42; see DISCUSSION). The examples in Fig. 11, *D* and *E* show the same data shown in Fig. 11, *B* and *C*, but this time the second spike in any doublet was deleted and the resulting "edited" frequencygram was fitted to the EMG profile as was done for other motoneurons. Once the doublets were deleted, a very good fit was obtained. The VI EMG profile accounted for 0.91 and 0.87, respectively, of the variance in the L2A33 frequencygram in Fig. 11, *D* and *E*.

### *Intracellular stimulation in acute experiment*

The finding that the frequency modulation of motoneurons generally mirrored the target muscle EMG envelope suggested to us that the filtered EMG might reproduce accurately a central driving function that would cause motoneurons to fire as they do. To test this notion we used digitally filtered EMG envelopes (from recordings obtained during normal walking) as templates to generate depolarizing currents that were applied intracellularly to lumbar motoneurons in a conventional anesthetized acute spinal cat preparation. Figure 12 shows an example of results obtained in a plantaris motoneuron.

We used as template the filtered EMG recorded from RF in *cat M* on *day 10*. By fine adjustments of the DC offset and input signal amplitude, we converged empirically on a combination of parameters that caused the output of the plantaris motoneuron to closely resemble the instantaneous frequencygram of motoneuron M5A10 (last trace in Fig. 12). Unit M5A10 had been recorded simultaneously with the RF EMG that was used as template. Its original frequencygram was displayed on an oscilloscope, as a guide to converge on the stimulation parameters. Note that the artificially generated burst and the naturally generated burst have similar shapes and also the peak frequencies reached for each burst are similar. The only discrepancies occurred at the end of the bursts, where it was not possible to obtain a more precise match.

In the same experiment, by making the DC

FIG. 11 (*continued*)

(note *thicker trace* and longer interspike intervals following doublets). *B* and *C*: displays of instantaneous frequencygrams for unit L2A33 at two treadmill speeds, 0.32 and 0.85 m/s. Note vertical calibration. Occurrences of initial doublets are shown by *circled data*. *D* and *E*: the same data of parts *B* and *C* are displayed after deleting the second spikes of initial doublets (see text). Note the close fit between the smoothed VI EMG and the edited frequencygrams.

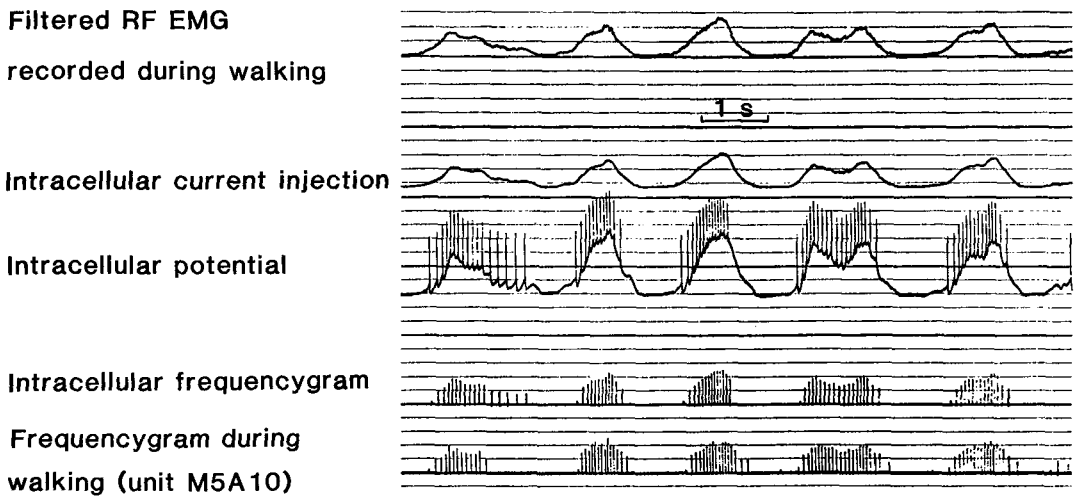


FIG. 12. Example of simulation of natural RF motoneuron discharge patterns by intracellular current injection in a plantaris motoneuron in an anesthetized cat. Further description in text.

bias more negative and increasing the phasic gain, we caused the plantaris motoneuron of Fig. 12 to fire bursts of action potentials that closely resembled the activity characteristic of the high-threshold motoneuron M11A10 (see Fig. 3), rather than the low-threshold motoneuron M5A10. Indeed, in several instances we were able to make an impaled lumbar motoneuron behave like either a low- or a high-threshold motoneuron during locomotion. The result of this experiment strongly suggested that *1*) the smoothed EMG recorded from a given muscle appeared to resemble closely the net synaptic drive that reached lumbar motoneurons during walking, and *2*) low- and high-threshold motoneurons in a given muscle appeared to receive the same common driving signal and to differ primarily in the absolute strength of their synaptic input and/or their intrinsic current threshold, which together determined their recruitment threshold.

## DISCUSSION

### *Close relationship between α-motoneuron frequencygrams and filtered EMG profiles of target muscles*

The most important general finding of this study was that for all anterior thigh α-motoneurons active during walking, the modulations in firing frequency closely resembled the modulations in the amplitude of the rectified filtered EMG recorded simultaneously from the appropriate target muscle. This finding has the following implications.

1. IN UNIFUNCTIONAL MUSCLES, A SINGLE LOCOMOTORY DRIVING FUNCTION IS EXPRESSED IN ALL ACTIVE α-MOTONEURONS. During locomotion at speeds between 0.1 and 1.3 m/s, every active motoneuron appears to be driven by the same net synaptic input as all other active motoneurons that innervate the same target muscle. No special modes of recruitment need to be postulated during walking. Active motoneurons appear to differ only in their intrinsic threshold and the synaptic strength derived from common sources controlling the entire pool. Evidence was provided by the comparable quality of the fits to frequencygrams of high-, medium-, and low-threshold motoneurons given by the target muscle EMG and also by the ability to replicate with intracellular stimulation the locomotory discharge patterns of low- or high-threshold motoneurons using the same EMG profile as current template.

Our terminology of "low-, medium-, or high-threshold" units is only meant to reflect their recruitment order within the limited population of units that are recruited at speeds of locomotion of up to 1.3 m/s. Therefore,

this conclusion is not necessarily in conflict with demonstrated differences in synaptic input of peripheral and central origin to slow- and fast-type motoneurons in mixed-type muscles (14, 26, 33). During locomotion up to 1.3 m/s, probably only type S and type FR motoneurons are recruited (18, 40, 41). It remains possible that different patterns of synaptic drive may be impressed onto yet higher-threshold type F motoneurons (4) that are likely called into action at greater levels of locomotory effort (e.g., fast trot, gallop) or in the performance of other tasks like jumping, paw shaking (37), or rapid postural adjustments (34, 35).

The finding of a single common drive applies to the unifunctional muscles VI, VM, VL, and also RF. The latter muscle provides an apparent paradox. The locomotory role of RF, often classified as a "hip flexor" (32), remains obscure. In reduced cat preparations the phase of the step cycle in which RF is active depends on the level of brain stem section. In intercollicularly decerebrated "mesencephalic" cats RF fires pure flexor bursts (9, 13, 32; S. Rossignol, personal communication). In decorticated cats, the phase of activity of RF can be completely reversed (from extension to flexion) by tonic exteroceptive input (32). In our recordings from normal cats, RF typically produced a single EMG burst per step cycle, during the stance phase (see Figs. 3, 5, and 12). On occasion, however, we also recorded a small EMG burst during swing, consistent with earlier reports for normal cats (8) and findings for decorticated cats during trotting (32). However, none of seven identified RF motoneurons was ever observed to fire extra spikes during swing. The origin of the swing-phase RF EMG remains a mystery. Possibly a separate population of motoneurons, from which we did not record single units, is responsible for the second burst, in analogy with sartorius (19, 28 and see below). Alternatively, only a few motoneurons might fire two bursts, but we did not encounter such units.

2. IN MULTIFUNCTIONAL MUSCLES, MOTONEURONS CAN BE CLASSIFIED INTO LOCOMOTORY TASK-DEPENDENT GROUPS. Motoneurons innervating sartorius (SA-a or SA-m) are functionally classified into three task-dependent groups that are independently activated during the step cycle. The special case of sartorius motoneurons is treated in detail in the following paper (19). For each group of motoneurons in SA, however, the same considerations regarding a single locomotory driving function apply as for the vasti and RF muscles.

3. THE FILTERED EMG PROFILE REFLECTS THE NET SYNAPTIC DRIVE TO A MOTONEURON POOL. The characteristic fluctuations in the amplitude of the smoothed EMG recorded from anterior thigh muscles appear to reflect ongoing changes in the strength of the net synaptic drive, rather than being dominated by random occlusions in the waveforms recorded simultaneously from many motor units or variability in the electrical coupling between EMG electrodes and muscle fibers. Evidence is provided by the close correlation typically found between fluctuations in EMG and in the frequencygram of individual motoneurons. For SA, the EMG profiles recorded from different muscle regions reflect a superposition of the activity of the corresponding motoneuron task groups (19).

A consequence of practical value is that EMG profiles recorded from unifunctional muscles can provide useful, accurate, and quite detailed moment-to-moment information about the net synaptic input to the motoneuron pool. Recording EMG from individual muscles is considerably easier than recording single motor units. Our results imply that the information content in the frequencygram of a single motoneuron and in the smoothed EMG profile of a unifunctional muscle are, for practical purposes, equivalent.

4. MOTONEURON FIRING PATTERNS DIFFER IN NORMAL AND DECEREBRATED CATS. The normal patterns of motoneuron activation are fundamentally different from patterns described earlier for hindlimb motoneurons of decerebrated cats (22, 42). In intercollicularly transected "mesencephalic" cat preparations made to walk on a moving belt by electrical stimulation in the brain stem, motoneurons typically fire uniform bursts consisting of a high-frequency (100–300 pps) initial doublet, following by a longer interpulse interval and a train of impulses at a fairly constant "preferred discharge rate" (36, 42). Similar observations apply to paralyzed mesencephalic cats in "fictive" locomotion (24), to higher-level "premammillary" decerebrated cat preparations that can walk spontaneously (22) and to curarized spinal cats injected with L-DOPA (7).

Zajac and Young (42) found that 80% of all hindlimb motoneurons fired initial doublets in most bursts during decerebrated cat locomotion at 0.45–1.34 m/s. Only 1 out of 70 recorded motoneurons was not ever observed to fire doublets. In contrast, we found that over 90% of all motoneurons did not fire doublets during normal cat locomotion at 0.1–1.3 m/s. For the 4/51 motoneurons that did, the incidence of doublets decreased at higher walking speeds.

This discrepancy cannot be attributed to a systematic difference in the motoneuronal subpopulations recorded. Doublets have been reported for flexor as well as extensor motoneurons in the $L_5$, $L_7$, and $S_1$ ventral roots (22, 24, 42). Motoneurons have been shown to be recruited in order of increasing CV in normal cats (18), which is the typical pattern of recruitment in decerebrated cats during stretch reflexes (3, 16) and presumably also during locomotion (41, 42). Instead, the underlying reason for the difference must lie in some other systematic change introduced by decerebration. For example, the recent finding that decerebration causes long-lasting changes in the intrinsic membrane properties of spinal motoneurons, leading to a sustained motor discharge in response to brief excitatory inputs (23), may also be related to the higher incidence of initial doublets found in decerebrated cats.

5. RELATIVE ROLES OF RATE CODING AND NEW RECRUITMENT IN NORMAL CAT LOCOMOTION. Deriving information on single motor-unit recruitment from recordings of whole muscle EMG alone is a notoriously difficult problem (e.g., 17, 29). Both the summation of motor-unit potentials contributing to a recorded EMG and the summation of motor-unit forces involve several complex nonlinearities. Surprisingly, however, the EMG-force relation can be fairly linear in human muscles for isometric constant effort over a wide range (29). Under these conditions, the rectified smoothed whole muscle EMG can provide a signal that varies in a simple relation to force, in spite of marked nonlinearities in the generation of the EMG.

In our experiments, the average and peak firing rates of most recorded motoneurons increased considerably for faster gaits. For individual active motoneurons, neither the value of the scaling constant, $K$, nor the coefficient of determination, $r^2$, changed appreciably with speed of gait. This means that the mean and peak frequency of individual motor units and the mean and peak EMG grew in parallel during normal cat locomotion up to a trot. However, we also observed that the recruitment thresholds of individual motor units were distributed throughout the whole range of EMG, at all speeds of locomotion tested. Therefore, the EMG activity grew not only in simple proportion to the increased firing rates of units that were recruited early, but also as a consequence of the recruitment of additional motor units. A surprisingly linear relationship between unit frequency and whole muscle EMG persisted over a wide range of effort, apparently as a result of just-sufficient increases in occlusion of the EMG.

The finding that higher-threshold motoneurons had consistently *lower* firing rates than lower-threshold motoneurons for matched speeds contradicts earlier findings on the "tonic" vs. "phasic" firing behavior of low- and high-threshold motoneurons in reduced preparations (10). It also highlights the apparent importance of rate coding in motoneurons with *lowest* recruitment threshold. Such units were often observed (Fig. 10) to reach and exceed 35 spikes/s even at 0.5 m/s (a modest speed of walking for a large male cat) and generally increased their peak discharge at the average rate of 10 spikes/s per additional 0.6 m/s increase in walking speed (Fig. 7*A*). The "textbook" notion that low-threshold cat motoneurons plateau at frequencies of ~10 pps (e.g., Ref. 12) is a serious misconception. Several studies of human motor-unit discharge during isometric contractions (6, 30, 31) also agree with our finding of substantial rate coding in cat hindlimb motoneurons.

ACKNOWLEDGMENTS

We thank M. J. Bak for assistance with the design and construction of microelectrodes, M. Chapman and M. Manley for training and caring after cats, and Dr. J. W. Fleshman for his help with intracellular experiments and valuable comments on this manuscript.

N. Sugano was supported by a Fogarty Visiting fellowship.

M. J. O'Donovan was supported by a Muscular Dystrophy Association postdoctoral fellowship.

Present address of J. A. Hoffer: Dept. of Clinical Neurosciences, University of Calgary, Faculty of Medicine, Calgary, Alberta T2N 4N1, Canada

Present address of N. Sugano: Dept. of Electronics, Faculty of Engineering, Tamagawa University, Tokyo 194, Japan.

Present address of M. J. O'Donovan: Dept. of Physiology and Biophysics, University of Iowa, Iowa City, IA 52242.

Reprint requests should be sent to J. A. Hoffer.

Received 18 December 1985; accepted in final form 5 September 1986.

## REFERENCES

1. BALDISSERA, F., CAMPADELLI, P., AND TESIO, L. Frequency coding in alpha-motoneurones of cat. *Brain Res.* 160: 155–158, 1979.
2. BALDISSERA, F. AND GUSTAFSSON, B. Supraspinal control of the discharge evoked by constant current in the alpha-motoneurones. *Brain Res.* 25: 642–644, 1971.
3. BAWA, P., BINDER, M. D., RUENZEL, P., AND HENNEMAN, E. Recruitment order of motoneurons in stretch reflexes is highly correlated with their axonal conduction velocity. *J. Neurophysiol.* 52: 410–420, 1984.
4. BURKE, R. E. Motor units: anatomy, physiology and functional organization. *Handbook of Physiology. The Nervous System II.* Bethesda, MD: Am. Physiol. Soc., 1981, chapt. 10, p. 345–422.
5. BURKE, R. E. AND RUDOMIN, P. Spinal neurons and synapses. In: *Handbook of Physiology. The Nervous System. Cellular Biology of Neurons.* Bethesda, MD: Am. Physiol. Soc., 1977, sect. 1, vol. 1, part 2, p. 877–944.
6. DELUCA, C. J., LEFEVER, R. S., MCCUE, M. P., AND XENAKIS, A. P. Behaviour of human motor units in different muscles during linearly varying contractions. *J. Physiol. Lond.* 329: 113–128, 1982.
7. EDGERTON, V. R., GRILLNER, S., SJOSTROM, A., AND ZANGGER, P. Central generation of locomotion in vertebrates. In: *Neural Control of Locomotion,* edited by R. M. Herman, S. Grillner, P. S. G. Stein, and D. G. Stuart. New York: Plenum, 1976, p. 439–464.
8. ENGBERG, I. AND LUNDBERG, A. An electromyographic analysis of muscular activity in the hindlimb of the cat during unrestrained locomotion. *Acta Physiol. Scand.* 75: 614–630, 1969.
9. GAMBARIAN, P. P., ORLOVSKY, G. N., PROTOPOPOVA, T. Y., SEVERIN, F. V., AND SHIK, M. L. The activity of muscles during different gaits and adaptive changes of moving organs in family Felidae. Morphology and ecology of Vertebrates. *Proc. Inst. Zool. Acad. Sci. USSR* 48: 220–239, 1971.
10. GRANIT, R., PHILLIPS, C. G., SKOGLUND, S., AND STEG, G. Differentiation of tonic from phasic alpha ventral horn cells by stretch, pinna, and crossed extensor reflexes. *J. Neurophysiol.* 20: 470–481, 1957.
11. GRILLNER, S. Locomotion in vertebrates: central mechanisms and reflex interaction. *Physiol. Rev.* 55: 247–304, 1975.
12. GRILLNER, S. AND UDDO, M. Motor unit activity and stiffness of the contracting muscle fibers in the tonic stretch reflex. *Acta Physiol. Scand.* 81: 422–424, 1971.
13. GRILLNER, S. AND ZANGGER, P. How detailed is the central pattern for locomotion? *Brain Res.* 88: 367–371, 1975.
14. GUSTAFSSON, B. AND PINTER, M. J. An investigation of threshold properties among cat spinal alpha-motoneurons. *J. Physiol. Lond.* 357: 453–483, 1984.
15. HENNEMAN, E. AND MENDELL, L. M. Functional organization of motoneuron pool and its inputs. *Handbook of Physiology. The Nervous System II.* Bethesda, MD: Am. Physiol. Soc., 1981, chapt. 11, p. 423–507.
16. HENNEMAN, E., SOMJEN, G., AND CARPENTER, D. O. Functional significance of cell size in spinal motoneurons. *J. Neurophysiol.* 28: 560–580, 1965.
17. HODGSON, J. A. The relationship between soleus and gastrocnemius muscle activity in conscious cats—a model for motor unit recruitment? *J. Physiol. Lond.* 337: 553–562, 1983.
18. HOFFER, J. A., LOEB, G. E., MARKS, W. B., O'DONOVAN, M. J., PRATT, C. A., AND SUGANO, N. Cat hindlimb motoneurons during locomotion. I. Destination, axonal conduction velocity, and recruitment threshold. *J. Neurophysiol.* 57: 510–529, 1987.
19. HOFFER, J. A., LOEB, G. E., SUGANO, N., MARKS, W. B., O'DONOVAN, M. J., AND PRATT, C. A. Cat hindlimb motoneurons during locomotion. III. Functional segregation in sartorius. *J. Neurophysiol.* 57: 554–562, 1987.
20. HOFFER, J. A., O'DONOVAN, M. J., AND LOEB, G. E. A method for recording and identifying single motor units in intact cats during locomotion. *Soc. Neurosci. Abstr.* 5: 1248, 1979.
21. HOFFER, J. A., O'DONOVAN, M. J., PRATT, C. A., AND LOEB, G. E. Recruitment order and firing patterns of identified cat hindlimb motor units during unrestrained treadmill walking. *Soc. Neurosci. Abstr.* 6: 761, 1980.
22. HOFFER, J. A., O'DONOVAN, M. J., PRATT, C. A., AND LOEB, G. E. Discharge patterns of hindlimb motoneurons during normal cat locomotion. *Science Wash. DC* 213: 466–468, 1981.
23. HOUNSGAARD, J., HULTBORN, H., JESPERSEN, B., AND KIEHN, O. Intrinsic membrane properties causing a bistable behaviour of alpha-motoneurones. *Exp. Brain Res.* 55: 391–394, 1984.
24. JORDAN, L. M. Factors determining motoneuron rhythmicity during fictive locomotion. In: *S.E.B. Symposia XXXVI: Neural Origin of Rhythmic Movements.* Cambridge, UK: Cambridge Univ. Press, 1983, p. 423–444.
25. JORDAN, L. M., PRATT, C. A., AND MENZIES, J. A. Locomotion evoked by brainstem stimulation: occurrence without phasic segmental afferent input. *Brain Res.* 177: 204–207, 1979.
26. KANDA, K., BURKE, R. E., AND WALMSLEY, B. Differential control of fast and slow twitch motor units in the decerebrate cat. *Exp. Brain Res.* 29: 57–74, 1977.
27. KERNELL, D. Rhythmic properties of motoneurones

innervating muscle fibres of different speed in m. gastrocnemius medialis of the cat. *Brain Res.* 160: 159–162, 1979.

28. LOEB, G. E., MARKS, W. B., AND HOFFER, J. A. Cat hindlimb motoneurons during locomotion: IV. Participation in cutaneous reflexes. *J. Neurophysiol.* 57: 563–573, 1986.
29. MILNER-BROWN, H. AND STEIN, R. B. The relation between the surface electromyogram and muscular force. *J. Physiol. Lond.* 246: 549–569, 1975.
30. MONSTER, A. W. Firing rate behavior of human motor units during isometric voluntary contraction: relation to unit size. *Brain Res.* 171: 349–354, 1979.
31. MONSTER, A. W. AND CHAN, H. Isometric force production by motor units of extensor digitorum communis muscle in man. *J. Neurophysiol.* 40: 1432–1443, 1977.
32. PERRET, C. Centrally generated pattern of motoneuron activity during locomotion in the cat. In: *S.E.B. Symposia XXXVI: Neural Origin of Rhythmic Movements.* Cambridge, UK: Cambridge Univ. Press, 1983, p. 405–422.
33. PINTER, M. J., BURKE, R. E., O'DONOVAN, M. J., AND DUM, R. P. Supraspinal facilitation of cutaneous polysynaptic EPSPs in cat medial gastrocnemius motoneurons. *Exp. Brain Res.* 45: 133–143, 1982.
34. RUSHMER, D. S., MACPHERSON, J. M., DUNBAR, D. C., AND RUSSELL, C. J. Responses of lateral gastrocnemius innervation subcompartments and soleus to paired perturbations of posture. *Soc. Neurosci. Abstr.* 9: 63, 1983.
35. RUSSELL, C. J., DUNBAR, D. C., RUSHMER, D. S., MACPHERSON, J. M., AND PHILLIPS, J. O. Differential activity of innervation subcompartments of cat lateral gastrocnemius during natural movements. *Soc. Neurosci. Abstr.* 8: 948, 1982.
36. SEVERIN, F. V., SHIK, M. L., AND ORLOVSKII, G. N. Work of the muscles and single motor neurones during controlled locomotion. *Biophysics* 12: 762–772, 1967.
37. SMITH, J. L., BETTS, B., EDGERTON, V. R., AND ZERNICKE, R. F. Rapid ankle extension during paw shakes: selective recruitment of fast ankle extensors. *J. Neurophysiol.* 43: 612–619, 1980.
38. STUART, D. G. AND ENOKA, R. Motoneurons, motor units, and the size principle. In: *The Clinical Neurosciences. Neurobiology,* edited by R. N. Rosenberg. New York: Churchill Livingstone, 1983, sect. 5, p. 471–517.
39. SUGANO, N., MARKS, W. B., HOFFER, J. A., FLESHMAN, J. W., AND LOEB, G. E. A close relationship between whole muscle EMG and the recruitment and firing rates of single motoneurons. *Soc. Neurosci. Abstr.* 8: 947, 1982.
40. WALMSLEY, B., HODGSON, J. A., AND BURKE, R. E. Forces produced by medial gastrocnemius and soleus muscles during locomotion in freely moving cats. *J. Neurophysiol.* 41: 1203–1216, 1978.
41. ZAJAC, F. E. AND FADEN, J. S. Relationship among recruitment order, axonal conduction velocity, and muscle unit properties of type-identified motor units in cat plantaris muscle. *J. Neurophysiol.* 53: 1303–1322, 1985.
42. ZAJAC, F. E. AND YOUNG, J. L. Discharge properties of hindlimb motoneurons in decerebrate cats during locomotion induced by mesencephalic stimulation. *J. Neurophysiol.* 43: 1221–1235, 1980.